Space–time focusing of Bessel-like pulses

M. Clerici,[1] D. Faccio,[1,*] E. Rubino,[1] A. Lotti,[1,2] A. Couairon,[2] and P. Di Trapani[1]

[1]*CNISM and Dipartimento di Fisica e Matematica, Università dell'Insubria, Via Valleggio 11, 22100 Como, Italy*

[2]*Centre de Physique Théorique, CNRS, École Polytechnique, F-91128 Palaiseau, France*

**Corresponding author: daniele.faccio@uninsubria.it*

Received June 21, 2010; revised August 16, 2010; accepted August 18, 2010;
posted September 9, 2010 (Doc. ID 130481); published September 28, 2010

We report on a space–time compression technique allowing for complete and independent control of the longitudinal dynamics and of the transverse pulse localization by means of spatial beam shaping. We experimentally observe both strong temporal compression and high transverse localization, of the order of a few wavelengths, along free-space propagation. © 2010 Optical Society of America

OCIS codes: 320.5520, 320.5540, 140.3300.

Controlling the temporal properties of a pulse by means of spatial shaping is fundamental for a number of fields related to light-matter interaction. For instance, active control of pulse temporal properties by spatial shaping has been employed for terahertz [1,2], high-harmonic, and attosecond pulse generation [3,4].

The propagation dynamics of space–time coupled wave packets has recently become a major issue of laser physics. For instance, it has been related to filamentation [5,6] and to the generation of single-cycle pulses and high-order harmonics [7,8].

The ability to actively control, through spatial shaping, the temporal properties of a pulse during its propagation is a promising tool for many applications. To date, the majority of proposals in this sense have relied on the use of tilted pulses (TPs) that are characterized by a temporal dynamics during free-space propagation (i.e., even in vacuum) that is due to the angular dispersion, i.e., to the spatial properties of the pulse [9–12]. However, one of the major drawbacks of these TP-based schemes is the intrinsic dependence of the spatial dynamics on the temporal dynamics, i.e., it is not possible to independently control the beam size and the pulse width, and a strong temporal compression always comes at the expense of a weak spatial localization [10,13].

In this Letter we report the experimental results obtained with a novel beam shaping technique relying on the temporal focusing of a conical wave (CW), i.e., the axisymmetric counterpart of the TP (see [14] for a review). The proposed technique allows for complete and independent control of the spatial localization at the compression position and of the pulse duration evolution.

CWs and TP share the same temporal dynamics, with the sole difference dictated by the different choice of the preferential axis identifying the temporal direction [15]. In Fig. 1 a sketch of the similarities and differences between TP and CW is shown. Note that for a CW, the spatial localization σ_b differs from the width σ_g of the Gaussian spatial apodizing envelope, while these two dimensions match, by definition, for a TP. In both cases the temporal dynamics is determined by the angular dispersion of the frequency components, i.e., by the tilt angle δ [9] and the width σ_g (FWHM) of the Gaussian spatial apodizing envelope [10]. The novelty introduced by considering CWs instead of TPs comes from the fact that the axial interference of the conical components induces a Bessel-shaped profile with width σ_b (FWHM) that can easily reach the wavelength limit or less [16] (see Fig. 1). This localization does not influence the temporal dynamics and can be varied by tuning the CW cone angle θ of the carrier wavelength λ as follows from the relation:

$$|J_0(\pi\sigma_b \sin(\theta)/\lambda)|^2 = 1/2. \tag{1}$$

We have experimentally verified the possibility of controlling the pulse temporal compression and a simultaneous spatial localization down to few wavelengths by the spatiotemporal focusing of a CW. The sketch of the setup is shown in Fig. 2.

An input 1 mJ, 1.5 cm beam width (FWHM), 800 nm Gaussian pulse with a spectral bandwidth supporting a transform limited 30 fs (FWHM) pulse duration, delivered by a Ti:sapphire laser source (Trident, Amplitude Technologies, France), is focused by means of a spherical mirror of focal length $f_1 = 2.5$ m. After the mirror, two different axicon (conical lens), ax_1 and ax_2, are inserted in the beam path in order to introduce radially symmetric frequency angular dispersion.

By properly choosing axicon of different materials and with different base angles, it is possible to cancel the carrier wavevector angle, thus creating a collimated ring with a strong angular dispersion. The distance d between the two axicon determines the output ring radius.

For the experiment we used a fused silica, 20° base angle, first axicon ax_1, and an SF11, 12.3° base angle, second axicon ax_2. The distance d was set at 8 cm.

Because of the initial beam focusing, the radially symmetric angular dispersion out of the two-axicon system translates, in the focal plane of the first mirror, i.e., at $z = f_1$, into a radially symmetric spatial chirp, and the beam is ring shaped with a central radius of nearly

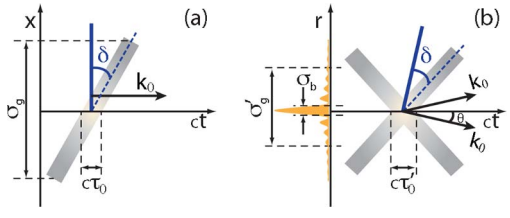

Fig. 1. (Color online) Comparison between (a) TP and (b) CW in the reference frame moving at each pulse group velocity. The dashed/solid blue lines represent the amplitude/phase fronts, respectively.

 © 2010 Optical Society of America

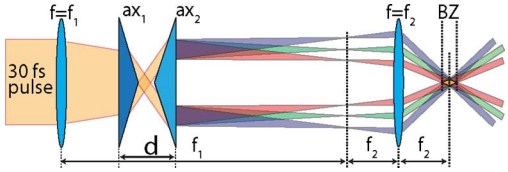

Fig. 2. (Color online) Sketch of the experimental layout. $f_1 = 250$ cm, $f_2 = 15$ cm, and $d = 8$ cm. ax_1 and ax_2 are the two axicon of base angle 20° and 12.3° made of fused silica and SF11, respectively.

12 mm. Finally, an $f_2 = 15$ cm BK7 focal lens, placed at a distance f_2 from the focal plane of the first lens, focuses the chirped pulse, generating the axial interference of the conical components, and hence a Bessel-shaped pulse, in a propagation region called the Bessel zone (BZ) around the lens focus. In our experimental condition the BZ was nearly 6 mm long. In order to characterize the spatial properties of the focused pulse and the temporal dynamics inside the BZ, we performed a spatially resolved cross correlation in a second-order nonlinear crystal (BBO, 10 μm thickness), i.e., a 3D-mapping [17], at different z coordinates of the BZ. The extremely short gate pulse, namely 7 fs, was obtained by compressing the spectral broadened radiation out of an argon-filled capillary [18] and was separately characterized by an interferential frequency resolved optical gating [19].

The experimental results are reported in Fig. 3. The spatial intensity profile $I(x, y)$ in Fig. 3(a) is a slice of a 3D mapping result at the temporal position of the pulse peak intensity and for a z coordinate corresponding to the center of the BZ. Note the nearly 3.7 μm width of the central peak that demonstrates the extreme spatial localization. From our measurements this localization remains almost invariant for the whole BZ (data not shown). In Fig. 3(b) a spatiotemporal slice, $I(y, t)$, of the same measure is reported. Finally, in Fig. 3(c) the evolution of the FWHM pulse duration inside the BZ is shown. It is clear that the pulse duration shrinks during the propagation while the temporal oscillations are due to diffraction from the axicon system edges. By adjusting the laser grating compressor, we were able to measure down to 29 ± 6 fs pulse duration (FWHM), which is compatible to that of a transform limited pulse with the available bandwidth. Note also that the maximum compression is obtained at the end of the BZ. This is a

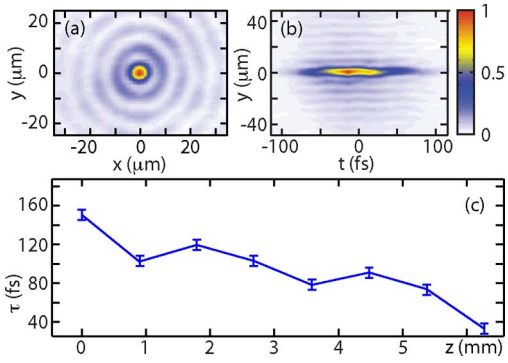

Fig. 3. (Color online) Experimental results. (a), (b) Spatial and spatiotemporal intensities of the focused CW at the center of the BZ, i.e., ~3 mm, respectively. (c) Pulse duration evolution inside the BZ.

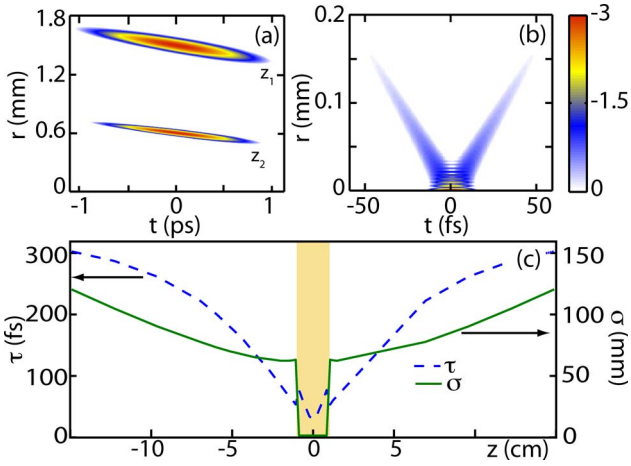

Fig. 4. (Color online) (a), (b) Logarithmic intensity profiles of a focusing CW. In (a) $z_1 = 0$ cm and $z_2 = 6$ cm from the $f_2 = 15$ cm lens. In (b) the pulse is in the focus. (c) Evolution of the pulse duration τ and beam width σ at FWHM (blue dashed and green solid curves, respectively) along the propagation. f_2 is at $z = -15$ cm from the center of the BZ (shaded region).

consequence of an additional phase term in the back focal plane of f_2 due to the positioning of the two-axicon system after f_1.

To quantify the temporal dynamics associated to the pulse focusing, we introduce the compression factor $\gamma(z) \equiv \tau(z)/\tau_0$, where τ is the temporal pulse duration (FWHM) at a distance z from the focusing lens, while τ_0 is the shortest pulse duration achieved during the focusing. We note that, because of the small ~4.5°, average cone angle, the geometrical correction linking τ_0 to τ_0' (as in Fig. 1) is negligible.

The specific choice of the experimental parameters for the proposed setup influences both the temporal and the spatial behavior of the focusing CW. For instance, by changing the distance between the two axicon, it is possible to control the carrier cone angle of the CW in the focal plane of f_2, thus controlling the spatial localization according to Eq. (1). On the other hand, the temporal evolution can be analytically described, as reported in Eqs. (3)–(5) of [10]. Specifically, increasing the input Gaussian beam width or increasing the tilt angle of the CW, e.g., by reducing the magnification f_2/f_1 of the telescope, will increase the compression factor γ. It is thus clear that the proposed system allows for an independent control over the temporal dynamics and spatial localization. In addition, note that for the chosen set of parameters, the value of γ within the BZ is more than 5. In contrast, a TP of 3.7 μm width, featured by a tilt angle of nearly 10°, similar to the experiment, would exhibit no appreciable temporal dynamics. For the sake of clarity we illustrate the results of focusing a spatially chirped ring pulse by means of a numerical simulation obtained with a linear, nonparaxial, spectral propagator, assuming the thin-lens approximation. The results are reported in Fig. 4, for input parameters compatible to our experimental setting.

In Fig. 4(a) the spatiotemporal intensity of the pulse at $z_1 = 0$ cm and $z_2 = 6$ cm far from the lens is reported in logarithmic scale, respectively, while in Fig. 4(b) the same is shown at the focus. It is clear that the pulse

shrinks both spatially and temporally as it propagates toward the focus, a Bessel modulation appears on axis and the pulse is X shaped. In Fig. 4(c) the beam width σ (FWHM) and the pulse duration τ are shown with solid and dashed curves, respectively. Note that, when the conical components start to interfere on axis, i.e., in the BZ (shaded region), the beam width suddenly decreases to the ~ 3.7 μm value, while the temporal dynamics is featured by a further compression of nearly $\gamma = 3$, not achievable with such a spatial localization in the TP configuration. We point out that, in order to obtain a quantitative agreement with the experimental measurements, some of the assumptions underlying the numerical results here reported have to be removed, for instance, the thin-lens approximation, and also the propagation through the two-axicon system should be fully modeled. Note that the pulse duration in the numerical simulation reaches a minimum at the center of the BZ, while in the experimental results of Fig. 3(c) the already mentioned residual phase term imposes a shift of the compression point at the end of the BZ.

In conclusion, we have proposed an experimental technique aimed at control of the temporal pulse dynamics with an independent control of the spatial localization. The results reported here demonstrate the possibility of achieving high values of temporal compression with a simultaneous strong spatial localization.

The authors acknowledge support from the Consorzio Nazionale Interuniversitario per le Scienze Fisiche della Materia, project INNESCO. M. C. acknowledges Gintaras Valiulis for fruitful discussions. D. F. acknowledges technical support from M. Petrovich and D. Richardson, ORC, Southampton (UK).

References

1. A. Stepanov, J. Kuhl, I. Kozma, E. Riedle, G. Almási, and J. Hebling, Opt. Express **13**, 5762 (2005).
2. J. M. Manceau, A. Averchi, F. Bonaretti, D. Faccio, P. D. Trapani, A. Couairon, and S. Tzortzakis, Opt. Lett. **34**, 2165 (2009).
3. S. Kazamias, F. Weihe, D. Douillet, C. Valentin, T. Planchon, S. Sebban, G. Grillon, F. Augé, D. Hulin, and P. Balcou, Eur. Phys. J. D **21**, 353 (2002).
4. D. Faccio, C. Serrat, J. M. Cela, A. Farrés, P. D. Trapani, and J. Biegert, Phys. Rev. A **81**, 011803 (2010).
5. M. Kolesik, E. M. Wright, and J. V. Moloney, Phys. Rev. Lett. **92**, 253901 (2004).
6. D. Faccio, M. A. Porras, A. Dubietis, F. Bragheri, A. Couairon, and P. Di Trapani, Phys. Rev. Lett. **96**, 193901 (2006).
7. S. Akturk, A. Couairon, M. Franco, and A. Mysyrowicz, Opt. Express **16**, 17626 (2008).
8. M. B. Gaarde and A. Couairon, Phys. Rev. Lett. **103**, 043901 (2009).
9. O. E. Martinez, J. P. Gordon, and R. L. Fork, J. Opt. Soc. Am. A **1**, 1003 (1984).
10. S. Zeng, D. Li, X. Lv, J. Liu, and Q. Luo, Opt. Lett. **32**, 1180 (2007).
11. D. Oron, E. Tal, and Y. Silberberg, Opt. Express **13**, 1468 (2005).
12. G. Zhu, J. van Howe, M. Durst, W. Zipfel, and C. Xu, Opt. Express **13**, 2153 (2005).
13. D. Li, X. Lv, S. Zeng, and Q. Luo, Opt. Lett. **33**, 128 (2008).
14. H. E. Hernández-Figueroa, M. Zamboni-Rached, and E. Recami, eds., *Localized Waves* (Wiley-Interscience, 2008).
15. M. Porras, G. Valiulis, and P. D. Trapani, Phys. Rev. E **68**, 016613 (2003).
16. F. Courvoisier, P.-A. Lacourt, M. Jacquot, M. K. Bhuyan, L. Furfaro, and J. M. Dudley, Opt. Lett. **34**, 3163 (2009).
17. P. D. Trapani, G. Valiulis, A. Piskarskas, O. Jedrkiewicz, J. Trull, C. Conti, and S. Trillo, Phys. Rev. Lett. **91**, 093904 (2003).
18. M. Nisoli, S. D. Silvestri, O. Svelto, R. Szipöcs, K. Ferencz, C. Spielmann, S. Sartania, and F. Krausz, Opt. Lett. **22**, 522 (1997).
19. G. Stibenz and G. Steinmeyer, Opt. Express **13**, 2617 (2005).